Organometallics 1992, *11*, 2514-2521

Synthesis and 2D NMR Studies of {Bis(pyrazolyl)borato}rhodium(I) Complexes with Weak Rh···H···C Interactions and the X-ray Crystal Structure of {(Cyclooctane-1,5-diyl)bis(pyrazol-1-yl)borato}(1,5-cyclooctadiene)rhodium

Massimo Bortolin, Urs E. Bucher, Heinz Rüegger, and Luigi M. Venanzi*

Laboratorium für Anorganische Chemie, Eidgenössische Technische Hochschule, Universitätstrasse 6, CH-8092 Zürich, Switzerland

Alberto Albinati and Francesca Lianza

Istituto di Chimica Farmaceutica dell' Università di Milano, Viale Abruzzi 42, I-20131 Milano, Italy

Swiatoslaw Trofimenko

Du Pont Electronics Department, Experimental Station, Wilmington, Delaware 19898

Received November 4, 1991

The novel rhodium(I) complexes [Rh{BBN(3-R-pz)$_2$}(LL)] (LL = 2 CO, COD (1,5-cyclooctadiene), and NBD (norbornadiene); R = H and CH_3; pz = 1-pyrazolyl; BBN = 9-borabicyclo[3.3.1]nonane) were synthesized and characterized in solution by one- and two-dimensional multinuclear NMR spectroscopy. The ^{1}H NMR spectra of all the compounds show that one of the methine protons (H$^{1'}$) of the BBN moiety is considerably deshielded. Furthermore, their three-dimensional solution structures, as derived by ^{1}H-NOESY spectroscopy, show that this proton is placed in proximity to the rhodium center. This is confirmed by the X-ray solid-state structure of [Rh{BBN(pz)$_2$}(COD)] (space group *Pnma*, a = 12.940 (2), b = 13.697 (2), c = 11.959 (2) Å; Z = 4; R = 0.034, R_w = 0.041 for 1485 observed reflections), which shows that the Rh–H8 (corresponding to H$^{1'}$ above) separation in this compound is 2.42 (4) Å. This interaction can be described as "agostic", albeit of the weak type, and might make a contribution to the lack of the inversion of the boatlike Rh(NN)$_2$B ring which, however, is characteristic for the complexes [Rh{Ph$_2$Bpz$_2$}(LL)] (LL = 2CO, NBD, and COD).

Introduction

Divalent metal ions of the first transition as well as other transition series form a wide variety of organometallic compounds with bis(pyrazolyl)borate anions $[R_2B(pz)_2]^-$ (R = H, alkyl, or aryl).[1-3] Ligands of this type, containing two alkyl or aryl substituents on the boron atom, are particularly interesting because they form stable four- and six-coordinate complexes with metal centers having a noninert gas configuration,[1-3] e.g., the molybdenum(II) complexes [Mo{Et$_2$B(pz)$_2$}(η^3-All)(CO)$_2$] (All = C_3H_5, 2-PhC_3H_4, and C_7H_7).[1c,2,3] A characteristic feature of these compounds, as well as many other coordinatively unsaturated species, is the presence of a strong interaction between the metal center and one CH group. Thus, the hydrogen-molybdenum distances in the latter two complexes above have been calculated to be as short as ca. 2.15 Å and ca. 1.93 Å, respectively, and for the C_3H_5 complex, a distance of 2.24 (2) Å has been found from X-ray data.[2] This M–H interaction was explained by Cotton and co-workers[3] as strong three-center two-electron bonding. It is now generally referred to as "agostic bonding".[4]

The C–H bonds involved in interactions of this type show some unusual spectroscopic properties. Thus, the infrared stretching vibrations are lower than usual and found at approximately 2700 cm^{-1}, e.g., at 2704 and 2664 cm^{-1} for [Mo{Et$_2$B(pz)$_2$}(η^3-C_3H_5)(CO)$_2$],[1c] while their ^{1}H NMR resonances are considerably shifted to high field, e.g., δ = −2.4 ppm, in the octahedral molybdenum complex A.[1c]

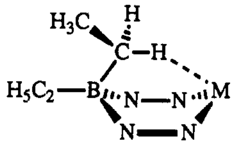

(A)

Weaker C–H–M interactions have also been reported[5] for compounds where the observed H–M distances are of the order of ca. 2.5 Å. However, here one finds strong deshielding of the protons interacting with the metal. Nevertheless, it has been proposed[5] that this kind of interaction is related to agostic bonding.

A C–H interaction of the latter type has been reported for the square planar complex [Ni{Et$_2$B(pz)$_2$}$_2$].[1b,d] It has also been found that this compound is considerably more

---

[1] (a) Trofimenko, S. *J. Am. Chem. Soc.* **1967**, *89*, 3170. (b) Trofimenko, S. *J. Am. Chem. Soc.* **1967**, *89*, 6288. (c) Trofimenko, S. *Acc. Chem. Res.* **1971**, *4*, 17.

[2] (a) Trofimenko, S. *J. Am. Chem. Soc.* **1968**, *90*, 4754. (b) Trofimenko, S. *Inorg. Chem.* **1970**, *9*, 2493.

[3] (a) Cotton, F. A.; Jeremic, M.; Shaver, A. *Inorg. Chim. Acta* **1972**, *6*, 543. (b) Cotton, F. A.; Day, V. W. *J. Chem. Soc., Chem. Commun.* **1974**, 415. (c) Cotton, F. A.; LaCour, T.; Stanislowski, A. G. *J. Am. Chem. Soc.* **1974**, *96*, 754. (d) Cotton, F. A.; Luck, R. L. *Inorg. Chem.* **1989**, *28*, 3210.

[4] (a) Brookhart, M.; Green, M. L. H. *J. Organomet. Chem.* **1983**, *250*, 395. (b) Brookhart, M.; Green, M. L. H.; Wong, L. L. *Prog. Inorg. Chem.* **1988**, *36*, 1.

[5] (a) Albinati, A.; Pregosin, P. S.; Wombacher, F. *Inorg. Chem.* **1990**, *29*, 1812. (b) Anklin, C. G.; Pregosin, P. S. *Magn. Reson. Chem.* **1985**, *23*, 671. (c) Albinati, A.; Anklin, C. G.; Ganazzoli, F.; Rüegg, H.; Pregosin, P. S. *Inorg. Chem.* **1987**, *26*, 503. (d) Albinati, A.; Arz, C.; Pregosin, P. S. *Inorg. Chem.* **1987**, *26*, 508.

0276-7333/92/2311-2514$03.00/0

stable against oxidation than its corresponding bis(hydrido)borate analogue [Ni{$H_2B(pz)_2$}$_2$].[1b] This stabilizing effect was originally attributed to agostic interactions[1b] but more recently, this reactivity difference has been attributed to steric blocking.[4a,6] Also LCAO–MO calculations indicate that there is no significant Ni–H interaction in [Ni{$Et_2B(pz)_2$}$_2$].[7] However, NMR data leave no doubt that, in solution, there is preferential interaction between one of the CH_2 groups (δ = 3.7 ppm) and the nickel atom in this complex.[1b] Interestingly, this additional stability is not observed for complexes with tetrahedral coordination geometries, e.g., for the pairs [Mn{$Et_2B(pz)_2$}$_2$]/[Mn{$H_2B(pz)_2$}$_2$][1b] and [Fe{$Et_2B(pz)_2$}$_2$]/[Fe{$H_2B(pz)_2$}$_2$].[1b]

Recently the synthesis of the new bis(pyrazolyl)borate ligand 1, containing the 9-borabicyclo[3.3.1]nonane (BBN) fragment, was reported.[8] This ligand forms stable complexes with a number of transition metal ions. An X-ray crystallographic study of [Co{BBN(pz)$_2$}$_2$] shows the presence of two agostic interactions, each involving the hydrogen atom on one of the methine carbons and cobalt, which can, therefore, be considered as having pseudooctahedral coordination. However, as this complex is paramagnetic, its NMR spectrum consists only of broad lines.[9] In order to correlate X-ray structural and NMR data, the compounds [Rh{BBN(3-R-pz)$_2$}(LL)] (R = H and CH_3; LL = 2CO, norbornadiene (NBD), and cyclooctadiene (COD)) were prepared, their solution structures were established by NMR, and the X-ray solid-state structure of [Rh{BBN(pz)$_2$}(COD)] was determined. Finally, the spectroscopic characteristics of these complexes were compared with those of the analogous derivatives containing the ligand 3, where the BBN fragment has been replaced by a diphenylboron moiety.

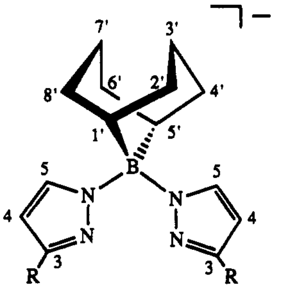

1 : R = H
2 : R = CH_3

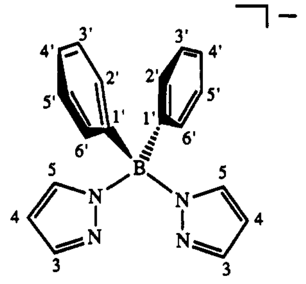

3

Results and Discussion

Synthesis. Ligands. The potassium salts of ligands 1 and 2 were prepared according to eq 1.

$$[\{BBN\}H]_2 + 4(3\text{-}R\text{-}pzH) + 2KOH \rightarrow 2K[BBN(3\text{-}R\text{-}pz)_2] + 2H_2O + 2H_2 \quad (1)$$

The critical step was the removal of the water produced. For this purpose a CaH_2-filled Soxhlet column was employed instead of the Dean–Stark trap used in earlier preparations.[8] The white crystalline, air-stable salts, obtained in high yields by this method, are very soluble in DMSO and DMF, moderately soluble in THF, methanol, ethanol, and acetone, but insoluble in water, ether, and hydrocarbon solvents.

Scheme I

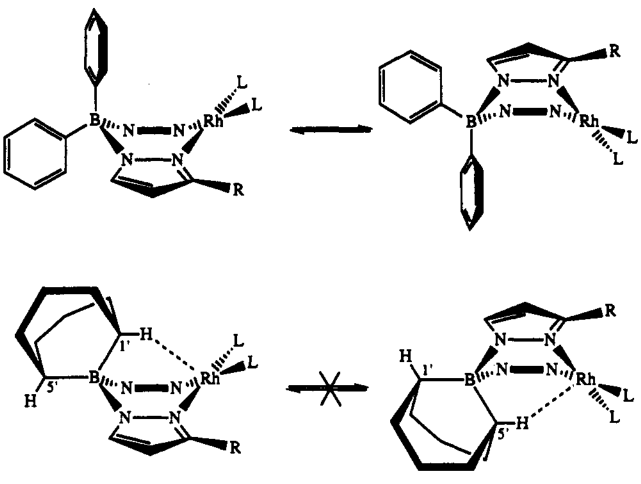

Complexes. The potassium salts of the appropriate bis(pyrazolyl)borate anions reacted with the rhodium complexes [$Rh_2Cl_2(LL)_2$] according to

$$[Rh_2Cl_2(LL)_2] + 2K[Y(3\text{-}R\text{-}pz)_2] \xrightarrow[CH_3CN]{-20\ °C} 2[Rh\{Y(3\text{-}R\text{-}pz)_2\}(LL)] + 2KCl \quad (2)$$

	Y	R	LL
4	BBN	H	2CO
5	BBN	H	NBD
6	BBN	H	COD
7	BBN	CH_3	2CO
8	BBN	CH_3	NBD
9	BBN	CH_3	COD
10	Ph_2B	H	2CO
11	Ph_2B	H	NBD
12	Ph_2B	H	COD

The products, obtained in moderate yields, are yellow to orange solids, stable under normal laboratory conditions.

Solution Studies. (a) NMR Spectra of Ligands 1–3. The ^1H, ^{13}C, and ^{15}N NMR data are consistent with the three ligands having C_{2v} symmetry, i.e., both pyrazole rings appear as magnetically equivalent, as do the phenyl groups in 3 and each pair of carbon atoms in α-, β-, and γ-positions to the boron atom in the BBN fragment. A full report on these and related pyrazolylborate ligands will be published elsewhere.[10]

(b) NMR Spectra of Rhodium(I) Complexes. Carbon and proton NMR evidence (Tables I–III) shows that the C_{2v} symmetry of ligand 3 is preserved in the compounds [Rh{$Ph_2B(pz)_2$}(LL)], 10–12. Thus, in [Rh{$Ph_2B(pz)_2$}(COD)] (12) one finds by ^1H and ^{13}C NMR spectroscopy only one type of phenyl substituent and only a single resonance for the olefinic CH unit at room temperature. As it is known from X-ray work that in the solid state the Rh(NN)$_2$B chelate ring in bis(pyrazolyl) complexes has a static boat conformation, the NMR data for 12 can be rationalized by assuming fast inversion of this ring on the NMR time scale (see Scheme I).

On the other hand, in the complexes [Rh{BBN(pz)$_2$}(LL)], 4–9, the 9-borabicyclo[3.3.1]nonane moiety gives rise to a total of five aliphatic carbon resonances having relative integrals of 1:2:2:2:1, for the 1′-, 2′ + 8′-, 3′ + 7′-, 4′ + 6′, and 5′-positions, respectively. Those of compound [Rh{BBN(pz)$_2$}(CO)$_2$] (4) are shown in the ^{13}C-coupled inverse

---

[6] (a) Echols, H. M.; Dennis, D. *Acta Crystallogr.* **1974**, *B30*, 2173. (b) Echols, H. M.; Dennis, D. *Acta Crystallogr.* **1976**, *B32*, 1627.

[7] Saillard, J. Y.; Hoffmann, R. *J. Am. Chem. Soc.* **1984**, *106*, 2006.

[8] Trofimenko, S.; Calabrese, J. C.; Thompson, J. S. *Angew. Chem.* **1989**, *102*, 207.

[9] Trofimenko, S.; Hulsbergen, F. B.; Reedijk, J. *Inorg. Chim. Acta* **1991**, *183*, 203.

[10] Manuscript in preparation.

Table I. ^{1}H NMR Data for Compounds 4–9[a]

	4[b]	5	6	7[b]	8	9
			Pyrazole Ring			
$\delta(H^5)$	7.62 d	7.47 d	7.51 d	7.51 d	7.31 d	7.41 d
$\delta(H^4)$	6.14 t	5.99 t	6.02 t	5.93 d	5.66 d	5.74 d
$\delta(H^3,CH_3)$	7.48 d	7.02 d	7.25 d	2.41 s	2.24 s	2.42 s
$J(H^5,H^4)$	2.28	2.19	2.23	2.22	2.11	2.19
$J(H^4,H^3)$	2.05	1.98	2.03			
			9-BBN Ring			
$\delta(CH^{1'})$	2.73 br	3.81 br	4.53 br	3.07 br	5.03 br	5.45 br
$\delta(CH^{5'})$	1.37 br	1.29 br	1.31 br	1.32 br	1.30 br	1.25 br
$\delta(CH)^{4'}$	2.06 m	2.02 m	2.08 m	2.14 m	2.07 m	2.20 m
$\delta(CH')^{4'}$	1.79 m	1.72 m	1.80 m	1.82 m	1.74 m	1.86 m
$\delta(CH^{2'})$	1.61 m	1.87 m	1.77 m	1.76 m	1.98 m	1.98 m
$\delta(CH'^{2'})$	1.14 m	1.10 m	1.35 m	1.39 m	1.54 m	1.78 m
$\delta(CH^{3'})$	1.88 m	1.79 m	1.93 m	1.93 m	1.71 m	2.07 m
$\delta((CH'^{3'})$	1.31 m	1.31 m	1.39 m	1.47 m	1.44 m	1.58 m
$J(C^{1'},H^{1'})$	109.1	110.6	110.0	110.7	108.1	110.9
$J(C^{5'},H^{5'})$	113.8	114.6	115.6	116.9	115.7	116.0
			Diene			
$\delta(CH^{1''})$		3.82 m	3.98 m		3.91 m	4.13 m
$\delta(CH^{2''})$		3.90 m	4.17 m		4.08 m	4.60 m
$\delta(CH^{3''})^{exo}$		3.85 m	2.47 m		3.94 m	2.48 m
$\delta(CH^{3''})^{endo}$			1.84 m			1.86 m
$\delta(CH^{4''})^{exo}$		1.22 m	2.38 m		1.13 m	2.45 m
$\delta(CH^{4''})^{endo}$			1.80 m			1.77 m
$\delta(CH^{5''})$		3.82 m			3.78 m	

[a] The spectra were recorded in $CDCl_3$ at room temperature. Chemical shifts (ppm) relative to $(CH_3)_4Si$ and coupling constants (Hz). Abbreviations used: for signal multiplicity s, singlet; br, broad singlet; d, doublet, dd, doublet of doublets, t, triplet; m, multiplet. Phenyl and 9-BBN carbons are labeled i, ipso; o, ortho; m, meta; p, para and α, β, and γ starting at the boron substitutions. [b] IR: $\nu_{(CO)}$ stretching bands (symmetric and asymmetric) for compound 4 appear at 2080 and 2015 cm^{-1} and for 7 at 2075 and 2013 cm^{-1}.

Table II. ^{13}C NMR Data for Compounds 4–9[a]

	4	5	6	7	8	9
			Pyrazole Ring			
$\delta(C^5)$	134.5	133.3	134.2	135.1	133.3	134.4
$\delta(C^4)$	104.8	103.5	104.4	104.5	103.8	104.7
$\delta(C^3)$	141.9	136.9	138.5	149.0	147.8	148.3
$\delta(CH_3)$				15.8	14.8	15.6
$J(Rh,C^3)$		2.21		2.03	1.76	
			9-BBN Ring			
$\delta(C^{1'})$	30.8	31.2	28.5	31.7	29.9	27.9
$\delta(C^{5'})$	20.1	20.7	20.05	20.9	21.7	22.2
$\delta(CH_2{}^{4'})$	32.2	32.3	32.9	32.2	32.1	32.4
$\delta(CH_2{}^{2'})$	30.3	30.5	30.9	30.5	30.9	30.7
$\delta(CH_2{}^{3'})$	24.3	24.4	25.0	24.3	24.3	24.5
			Diene			
$\delta(C^{1''})$	*b*	52.8	79.1	*c*	51.0	78.3
$\delta(C^{2''})$		54.7	81.1		53.5	77.5
$\delta(C^{3''})$		50.7	31.3		49.9	30.4
$\delta(C^{4''})$		61.1	31.2		61.1	30.1
$\delta(C^{5''})$					49.2	
$J(Rh,C^{1''})$	*b*	6.1	12.0	*c*	9.7	12.6
$J(Rh,C^{2''})$		9.7	13.7		10.8	13.2

[a] The spectra were recorded in $CDCl_3$ at room temperature: Chemical shifts (ppm) relative to $(CH_3)_4$ Si and coupling constants (Hz). [b] $\delta(CO) = 186.1$; $^{1}J(Rh,C) = 67.3$. [c] $\delta(CO) = 185.6$; $^{1}J(Rh,C) = 67.1$.

2D correlation,[11] which appears in Figure 1. Furthermore, in these complexes the protons on carbons 1′ and 5′ have very different chemical shifts, e.g., $\delta = 4.53$ and 1.32 ppm for compound **6**. Thus it must be concluded that, in the BBN complexes, the chelate ring conformation is static and that this conformational preference is strong, as there is *no indication* of a dynamic interchange at 100 °C in toluene-d_8. This preference might result from restricted flexibility of the BBN moiety imposed by its bicyclic nature, although a contribution from the interaction of one of the hydrogens of BBN with the metal center cannot be excluded. In this context it should be noted that conformational rigidity of $BBN(pz)_2$ has also been observed in some copper(I) complexes of the type $[Cu\{BBN(pz)_2\}(L)]$, L = CH_3CN or PPh_3,[10] where the hydrogen–copper interaction competes efficiently for the fourth coordination site.

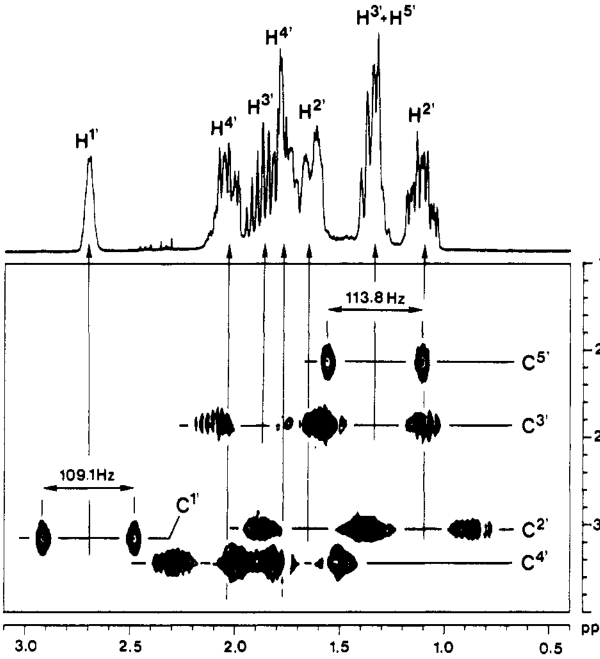

Figure 1. The ^{13}C–^{1}H (62.9/250 MHz) heteronuclear correlation experiment for $[Rh\{BBN(pz)_2\}(CO)_2]$ (**4**) showing (a) the assignment of the carbon and proton resonances and (b) the method for obtaining the $^{1}J(C,H)$ parameter.

In order to use the solution NMR data for a more de-

---

[11] (a) Summers, M. F.; Marzilli, L. G.; Bax, A. *J. Am. Chem. Soc.* **1986**, *108*, 4285. (b) Bax, A.; Griffey, R. H.; Hawkins, B. L. *J. Am. Chem. Soc.* **1983**, *105*, 7188.

Table III. ^{1}H and ^{13}C NMR Data for Compounds 10–12[a–c]

	^{1}H				^{13}C		
	10	**11**	**12**		**10**	**11**	**12**
			Pyrazole Ring				
$\delta(H^5)$	7.48 dd	7.37 dd	7.32 dd	$\delta(C^5)$	137.6	137.4	136.7
$\delta(H^4)$	6.26 t	6.14 t	6.10 t	$\delta(C^4)$	104.9	104.1	103.8
$\delta(H^3)$	7.66 d	7.41 d	7.06 d	$\delta(C^3)$	144.0	139.3	138.9
$J(H^5,H^4)$	2.4	2.44	2.28	$J(Rh,C^3)$	2.83		1.33
$J(H^3,H^4)$	2.09	1.94	1.91				
$J(H^5,H^3)$	0.54	0.44	0.45				
			Phenyl Ring				
				$\delta(C^i)$	148.0	149.8	148.8
$\delta(H^o)$	6.87 m	6.14 br	6.85 br	$\delta(C^o)$	133.9	134.3	133.9
$\delta(H^{m,p})$	7.26 m	7.27 m	7.29 m	$\delta(C^m)$	127.3	127.1	127.1
				$\delta(C^p)$	126.8	126.4	126.4
			Diene				
$\delta(H^{1''})$		3.85 br	3.57 m	$\delta(C^{1''})$	*d*	80.6	56.3
$\delta(H^{2''})$		3.85 br	3.57 m	$\delta(C^{2''})$		80.6	56.3
$\delta(H^{3''})$		2.16 br	3.52 m	$\delta(C^{3''})$		29.8	61.5
$\delta(H^{4''})$		1.59 m	1.13 s	$\delta(C^{4''})$		29.8	50.3
$\delta(H^{5''})$			3.52 m	$\delta(C^{5''})$			61.5
				$J(Rh,C^{1''})$	*d*	12.4	10.07
				$J(Rh,C^{3''})$			5.97
				$J(Rh,C^{4''})$			2.69

[a] The spectra were recorded in $CDCl_3$ at room temperature. Abbreviations as in Table I. [b] IR: $\nu_{(CO)}$ stretching bands (symmetric and asymmetric) for compound 10 appear at 2074 and 2013 cm^{-1}. [c] Compounds 10–12 show a $\delta(^{11}B)$ chemical shift of ca. 1 ppm relative to $BF_3\cdot OEt_3$. [d] $\delta(CO)$ = 185.3; $^1J(Rh,C)$ = 67.4.

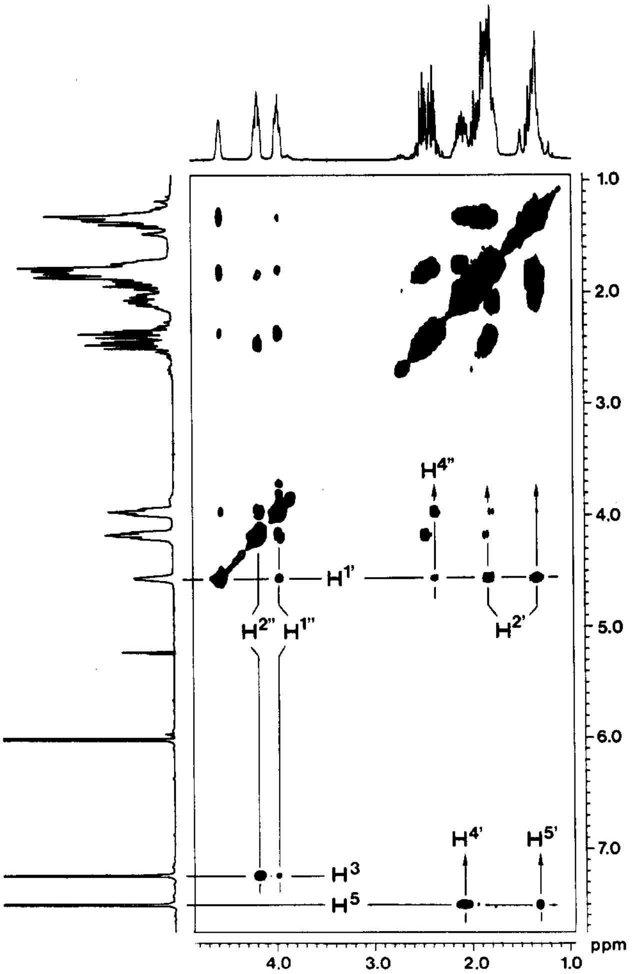

Figure 2. The 250-MHz 2D-NOESY spectrum for [Rh{BBN-$(pz)_2$}(COD)] (6), showing the spatial relationships between the different ligands.

tailed discussion of the structures of the complexes in solution, a complete assignment of the ^{1}H and ^{13}C resonances was carried out.

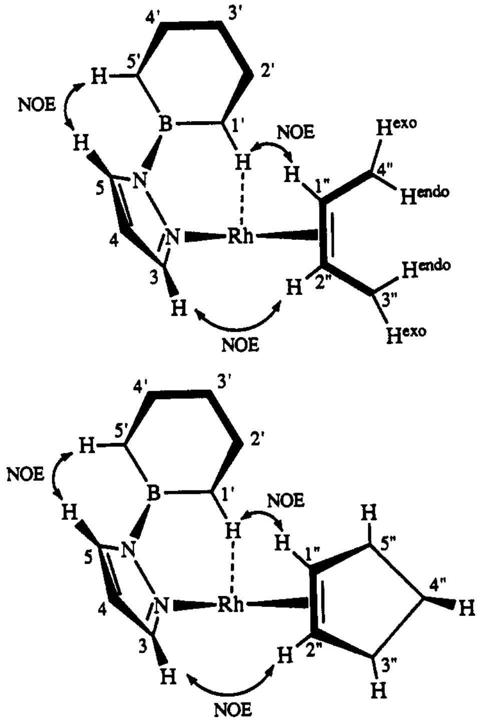

Figure 3. Schematic representation of the spatial relationship of the interacting atoms in the NOE spectra of **5** (top) and **6** (bottom).

Pyrazolyl Fragment. The assignment of the ^{1}H spectra followed entirely from two-dimensional nuclear Overhauser spectroscopy (NOESY[12]) (e.g., see Figure 2), showing proximity of H^5 to protons of the BBN entity (or the phenyl groups in 10–12), whereas H^3 is close in space to the olefinic units as in 5, 6, 11, and 12 (see the drawings of the half-molecules in Figure 3). The carbon spectrum was then assigned from the ^{1}H–^{13}C correlation experiment.

---

(12) Jeener, J.; Meier, B. H.; Bachmann, P. Ernst, R. R. *J. Chem. Phys.* **1979**, *71*, 4546.

9-BBN Fragment. Its reduced symmetry with respect to the free ligands 1 and 2, mentioned above, leads to inequivalence of the 1′- and 5′-, as well as 2′- and 4′-positions in the molecule, giving rise to five carbon signals. The ^{13}C–^{1}H correlation experiment (e.g., see Figure 1) relates these carbon signals to those of the hydrogens directly attached to them. In particular, as can be seen for $[Rh\{BBN(pz)_2\}(CO)_2]$ (4) in this figure, the 1′-carbon is related to a relatively deshielded proton resonance at δ = 2.73 ppm, while the 5′-carbon is associated with a proton in the expected range (δ = 1.37 ppm). The remaining carbon and hydrogen resonances were assigned from a combination of homo- (COSY[13]) and homonuclear (HMQC[11]) correlation spectroscopy, supported by two-dimensional Overhauser experiments described below.

Olefinic Ligand. The resonances of the cyclooctadiene and norbornadiene moieties were conveniently assigned by 2D ^{13}C–^{1}H correlation techniques after dealing with the lower symmetry via 2D-NOESY experiments, outlined in more detail below. A similar treatment was used for the phenyl groups in the complexes 10–12.

Aspects of the Solution Structure of the BBN Complexes 4–9. Having arrived at an unambiguous assignment of relevant protons in the molecules containing the BBN-derived ligands, one can proceed to discuss some aspects of the three-dimensional NMR solution structures of the complexes. It is now well established[14] that considerable insight into the spatial relationships of ligands in organometallic complexes can be derived from two-dimensional Overhauser spectroscopy. This is best illustrated here in the case of $[Rh\{BBN(pz)_2\}(COD)]$ (6) by considering the NOESY spectrum depicted in Figure 2 and the schematic drawing in Figure 3.

Starting with the pyrazolyl proton H^3, at δ = 7.25 ppm, as a convenient entry point into the system of ligands, the NOESY spectrum shows a cross peak to an olefinic proton resonating at δ = 4.17 ppm. Consequently, these two hydrogens have to be positioned on the same side of the rhodium coordination plane. The second olefinic proton (δ = 3.98 ppm) is in close proximity to the unique 1′-hydrogen of the BBN fragment, the latter proton showing additional close contacts to the BBN 2′-hydrogens, as expected, and also to the exo protons (4″) of the cyclooctadiene moiety. In a short triangulation, these observations allow positioning of the 1′-hydrogen approximately above the rhodium center. It should be noted here that the second 5′-hydrogen shows no NOE to olefinic protons and does not exchange slowly with the other methine protons via, for example, inversion of the $Rh(NN)_2B$ ring.

The particular location of the 1′-hydrogen of 9-BBN and the thermal stability of the $Rh(NN)_2B$ ring conformation indicate that there could be an agostic interaction[5] between a carbon–hydrogen bond and the rhodium.

Generally, three effects, observable by NMR spectroscopy, are recognized as being indicative for this type of bonding: (i) the value of the ^1H chemical shift, (ii) the reduction in the magnitude of the scalar coupling constant $^1J(C,H)$, and (iii) the presence of a scalar coupling to the metal nucleus for spin $I = {}^1/_2$ nuclei, ^{103}Rh, in our case.

While the values of δH are most easily accessible, their changes are not very well understood, as both considerable shielding[15] and deshielding[5] are observed. It is noteworthy that in compounds 4–9 deshielding is observed and that the chemical shifts of the proton in question increase when going from the carbon monoxide to the NBD and COD derivatives, e.g., from 2.73 to 3.81 and 4.53 ppm, for compounds 4–6, respectively. The 3-methylpyrazolyl, 7–9, derivatives show even higher deshielding (δ = 3.07, 5.03 and 5.45 ppm, respectively) when compared with their unsubstituted analogs.

Effects ii and iii are probably better understood: the C–H–M interaction should decrease the C–H bond order, and thus, $^1J(C,H)$ should decrease with increasing the M–H bond order. Using routine methods, the NMR parameters $J(C,H)$ and $J(Rh,H)$, are not readily extractable from the spectra of compounds 4–9 as (1) the broadness of the hydrogen resonances, due to unresolved couplings to other protons of the BBN fragment, precludes the direct observation of a rhodium coupling, and (2) the coupling constant $^1J(C,H)$ cannot be obtained from the proton-coupled ^{13}C spectrum as the resonances of the carbons in α-position to boron are broadened by partially relaxed coupling to the adjacent quadrupolar nucleus, thereby causing a considerable decrease of the signal-to-noise ratio.

However, there is now a very convenient way to obtain the $J(C,H)$ constants, i.e., by means of the heteronuclear correlation experiment using proton detection,[11] where this parameter can be read from the appropriate rows through the two-dimensional matrix (e.g., see Figure 1). It is found (see Table I) that the $^1J(C^{1'},H^{1'})$ values are approximately 110 Hz, slightly (but significantly in terms of errors involved) smaller than the corresponding values of ca. 116 Hz for $^1J(C^{5'},H^{5'})$ in complexes 4–9, as well as in ligands 1 and 2 (117.7 Hz).

The $J(Rh,H)$ values are even more difficult to obtain. Comparison of the width at half-height of the resonances due to $H^{1'}$ and $H^{5'}$, where the latter is resolved, indicates that $J(Rh,H)$ must be small. To obtain an estimate of these values a proton-detected rhodium–proton correlation, optimized for small coupling constants, was recorded. For $[Rh\{BBN(3\text{-}Me\text{-}pz)_2\}(COD)]$, (9) ($\delta(^{103}Rh)$ = 1205 ppm) this experiment showed correlation peaks between rhodium and (1) H^4,H^5 and the methyl of the pyrazolyl and (2) the olefinic and the exo protons of the BBN moiety. The absence of such a correlation peak for $H^{1'}$ may be either due to a vanishingly small coupling constant $J(Rh,H^{1'})$ with an upper limit of ca. 0.4 Hz or result from faster relaxation of the $H^{1'}$ proton in the relevant double- and zero-quantum terms compared to the pyrazolyl and olefinic protons.

The rather small (ca. 5%) reduction in $J(C,H)$ and the likely very small magnitude of $J(Rh,H)$, taken together, suggest that the observed interaction of the C–H bond with the metal is of the "pregostic" or weak interaction type (In this context *pregostic* can be understood either as *preagostic*, i.e., on the way to becoming agostic, or agostic of the weak type comprehensively described by Pregosin and co-workers.[5]). To support these findings from solution data, an X-ray crystal structure determination of $[Rh\{BBN(pz)_2\}(COD)]$ (6) in the solid state was carried out and is described below.

X-ray Crystal Structure of {(Cyclooctane-1,5-diyl)bis(pyrazol-1-yl)borato}(1,5-cyclooctadiene)rhodium (6). The crystals contain discrete molecules of $[Rh\{BBN(pz)_2\}(COD)]$ (6) separated by normal van der

---

[13] Rance, M.; Sørensen, O. W.; Bodenhausen, G.; Wagner, G.; Ernst, R. R.; Wüthrich, K. *Biochem. Biophys. Res. Commun.* **1983**, *117*, 458.

[14] (a) Albinati, A.; Ammann, C.; Pregosin, P. S.; Rüegger, H. *Organometallics* **1990**, *9*, 1826. (b) Rüegger, H.; Kunz, R. W.; Ammann, C. J.; Pregosin, P. S. *Magn. Reson. Chem.* **1991**, *29*, 197. (c) Ammann, C. J.; Pregosin, P. S.; Rüegger, H.; Albinati, A.; Lianza, F.; Kunz, R. W. *J. Organomet. Chem.* **1992**, *423*, 415.

[15] (a) Carr, N.; Dunne, B. J.; Orpen, A. G.; Spencer, J. L. *J. Chem. Soc., Chem. Commun.* **1988**, 926. (b) Cracknell, R. B.; Orpen, A. G.; Spencer, J. L. *J. Chem. Soc., Chem. Commun.* **1984**, 326; **1986**, 1005. (c) Arliguie, T.; Chaudret, B.; Jalon, F.; Lahoz, F. *J. Chem. Soc., Chem. Commun.* **1988**, 998. (d) Heddon, D.; Roundhill, D. M.; Fultz, W. C.; Rheingold, A. L. *Organometallics* **1986**, *5*, 336. (e) Koya, N.; Morokuma, K. *J. Am. Chem. Soc.* **1988**, *110*, 108.

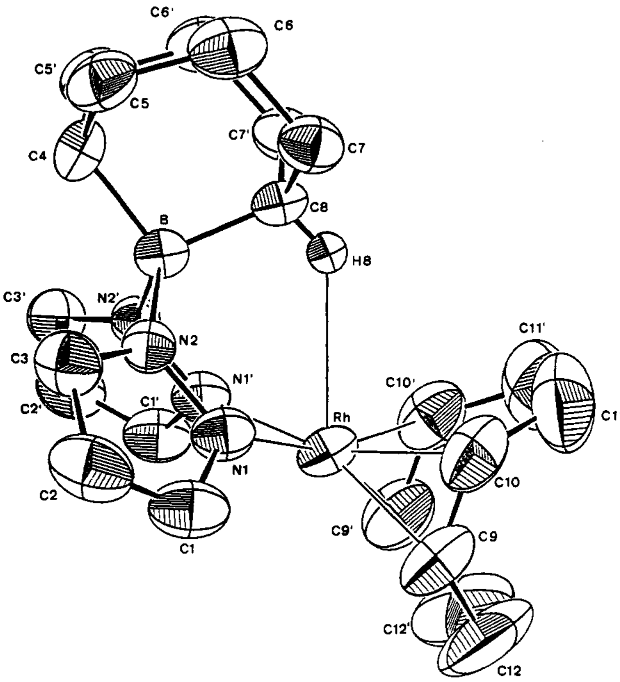

Figure 4. ORTEP view of the molecule $[Rh\{BBN(pz)_2\}(COD)]$ (**6**).

Table IV. Selected Bond Distances (Å) and Angles (deg) for $[Rh\{(C_8H_{14})B(pz)_2\}(COD)]$ (6) (Esd's in Parentheses)

Rh–N1	2.107 (3)	B–N2	1.590 (4)	C1–C2	1.373 (6)
Rh–C9	2.121 (5)	B–C4	1.620 (7)	C2–C3	1.364 (6)
Rh–C10	2.116 (5)	C8–H8	0.90 (4)	C9–C10	1.370 (7)
Rh–m^a	2.004 (5)	N1–C1	1.342 (5)	C10–C11	1.494 (8)
Rh–H8	2.42 (4)	N1–N2	1.360 (4)	C11–C11′^{b}	1.455 (8)
B–C8	1.575 (8)	N2–C3	1.383 (5)		

N1–Rh–N1′^{b}	86.5 (1)	C10–Rh–C10′	82.3 (2)
N1–Rh–C9	160.6 (2)	Rh–H8–C8	137. (3)
N1–Rh–C10	161.6 (1)	Rh–N1–N2	120.2 (2)
N1–Rh–C9′	92.3 (2)	N2–B–N2′	101.3 (3)
N1–Rh–C10′	92.7 (1)	N2–B–C8	112.6 (3)
N1–Rh–m^a	179.0 (1)	N2–B–C4	112.2 (3)
N1–Rh–m^a	92.7 (2)	B–C8–H8	110 (3)
m–Rh–m^a	88.2 (2)	B–N2–C3	131.7 (3)
C9–Rh–C9′	82.5 (2)		

^{a} *m* and *m′* are the midpoints of the bonds C9–C10 and C9′–C10′, respectively. ^{b} Primed atoms are related to those unprimed by the symmetry operation $x, y + {}^1/_2, z$.

Waals distances. An ORTEP view of the molecule is shown in Figure 4. A selection of relevant interatomic distances and bond angles is given in Table IV.

The molecule contains a crystallographic mirror plane going through the rhodium, boron, and bridgehead carbon atoms C4 and C8 of 9-BBN, rendering the two halves of the molecule equivalent. These have been denoted as primed and unprimed atoms in Figure 4 (It should be noted here that the atomic numbering employed for the crystal structure differs from that used for the discussion of the NMR spectra.). The coordination geometry at the rhodium atom can be regarded as square planar if only the two coordinated nitrogens and C═C bonds are considered. If one also takes into account the Rh–H8 interaction, then the complex should be described as square pyramidal. Interestingly, one finds that, as is common in complexes of this structure, the rhodium atom is placed slightly above the plane defined by the basal donor atoms N1 and N1′ and *m* and *m′* (these being the midpoints between C9 and C10 and C9′ and C10′, respectively; 0.01 Å).

The Rh–C9 and Rh–C10 distances must be considered as being equal given the values of the standard deviations (2.121 (5) and 2.116 (5) Å, respectively). These distances, as the other bonding parameters for the Rh–COD moiety, do not differ significantly from those found in the related compound $[Rh\{\eta^2\text{-}B(pz)_4\}(COD)]$ (**13**).[16]

The Rh–N distances (2.107 (3) Å) and the N1–Rh–N1′ bond angle (86.5 (1)°) are similar to the corresponding parameters in compound **13**, although the ligands in the two complexes are not identical. It should be noted here that in the pseudooctahedral complex $[Co\{BBN(pz)_2\}_2]$ (**14**) the analogous N–Co–N angles are 90.6 (1)° and 89.4 (1)°. However, all other bond lengths and angles in complex **6** agree well with those reported for compound **14**.

As found in this compound, the $Rh(NN)_2B$ heterocyclic ring is bent into a boatlike conformation, bringing the bridgehead H atom of 9-BBN, H8, in proximity to the rhodium center. This hydrogen atom could be located and refined, and the Rh–H8 (Rh–H$^{1'}$) separation is 2.42 (4) Å. Although this distance is shorter than the sum of the van der Waals radii of rhodium and hydrogen, it is relatively large when compared to reported typical metal–hydrogen separations of agostic type, which are in the range of 1.8–2.2 Å.[4] The Rh–H8 interaction, as mentioned earlier, is probably better described as weak interaction, of pregostic type, similar to those found in platinum and palladium complexes, e.g., *trans*-$[PtCl_2(benzoquinoline)(PEt_3)]$ (2.53 (8) Å), reported previously.[5a]

Conclusions

The solution and X-ray structural data obtained for the square planar rhodium complexes of bis(pyrazolyl)borate ligands of the type $\{BBN(3\text{-}R\text{-}pz)_2\}$ clearly show the presence of only weak M⋯H⋯C interactions in compounds of this type, in agreement with the recent LCAO–MO calculations on $[Ni\{Et_2B(pz)_2\}_2]$.[7] The hydrogen is directed here toward a filled metal orbital and is probably involved in a three-center four-electron bond of the type proposed for $[NPr^n_4]_2[PtCl_4]$-*cis*-$[PtCl_2(NH_2Me)_2]$,[17] as opposed to the situation in $[Mo\{Et_2B(pz)_2\}(\eta^3\text{-allyl})(CO)_2]$, where the metal forms a strong three-center two-electron bond because it needs electrons and gets them from the C–H bond.[2]

Experimental Section

Materials. Pyrazole and 9-borabicyclo[3.3.1]nonane were purchased from Fluka AG, and 3-methylpyrazole was obtained from Merck AG. They were used without further purification. Toluene (Puriss p.a. from Fluka AG) was used as such; tetrahydrofuran was freshly distilled from sodium hydride under an atmosphere of nitrogen. Hexane and acetonitrile were distilled from calcium hydride and stored over a molecular sieve (3 Å). The organometallic starting materials $[Rh_2Cl_2(CO)_4]$,[18] $[Rh_2Cl_2(COD)_2]$ (COD = cyclooctadiene),[19] and $[Rh_2Cl_2(NBD)_2]$ (NBD = norbornadiene)[20] were prepared as described in the appropriate references. Ligand **3** was available from an earlier study.[1b]

$K[\{C_8H_{14}\}B(3\text{-}R\text{-}pz)_2]$ (1, R = H; 2, R = CH_3). The appropriate pyrazole (17.02 g and 20.53 g for **1** and **2**, respectively; 0.250 mol) and KOH (7.01 g, 0.125 mol) were placed in a three-necked round-bottom flask equipped with a magnetic stirring bar, a thermometer, a serum stopper, and a Soxhlet extractor whose thimble was filled with ca. 15 g of CaH_2. Toluene (300 mL) was added, and the mixture was refluxed for 18 h at a bath temperature of 140 °C. The suspension containing a white precipitate

---

[16] Cocivera, M.; Ferguson, G.; Kaitner, B.; Lalor, F. J.; O'Sullivan, D. J.; Parvez, M.; Ruhl, B. *Organometallics* **1982**, *1*, 1132.

[17] Brammer, L.; Charnock, J. M.; Goggin, P. L.; Goodfellow, R. J.; Orpen, A. G.; Koetzle, T. F. *J. Chem. Soc., Dalton Trans.* **1991**, 1789.

[18] McCleverty, J. A.; Wilkinson, G. *Inorg. Synth.* **1966**, *8*, 211.

[19] Chatt, J.; Venanzi, L. M. *J. Chem. Soc.* **1957**, 4735.

[20] Abel, E. W.; Bennett, M. A.; Wilkinson, G. *J. Chem. Soc.* **1959**, 3178.

Table V. Microanalytical Data, Yields (%), and Melting Points of Compounds K[Y(3-R-pz)$_2$] (1–3) and [Rh{Y(3-R-pz)$_2$}(LL)] (4–12)

compd	Y	R	LL	yield, %	mp, °C	C[a]	H[a]	N[a]
1	BBN	H		79	>240	56.97 (57.15)	6.93 (6.85)	19.23 (19.04)
2	BBN	CH_3		75	>240	58.99 (59.63)	7.64 (7.51)	17.05 (17.38)
3	Ph_2B	H			>240	63.95 (63.91)	4.86 (4.77)	16.31 (16.56)
4	BBN	H	2CO	52	146–147[b]	46.21 (46.41)	5.00 (4.87)	13.62 (13.53)
5	BBN	H	NBD	60	234–236	55.74 (56.03)	6.16 (6.27)	12.60 (12.44)
6	BBN	H	COD	47	219–221	56.27 (56.68)	7.00 (6.92)	11.92 (12.00)
7	BBN	CH_3	2CO	64	156–158[b]	48.58 (48.90)	5.46 (5.47)	12.78 (12.67)
8	BBN	CH_3	NBD	55	210–212	56.06 (57.76)	6.77 (6.74)	11.13 (11.71)
9	BBN	CH_3	COD	42	226–228	57.68 (58.32)	7.38 (7.34)	11.25 (11.33)
10	Ph_2B	H	2CO	58	198–200[b]	52.39 (52.44)	3.57 (3.52)	12.36 (12.23)
11	Ph_2B	H	NBD	57	>240	60.43 (60.76)	5.04 (4.89)	11.44 (11.34)
12	Ph_2B	H	COD	81	237–239	60.88 (61.20)	5.62 (5.53)	11.06 (10.98)

[a] Calculated values are given in parentheses. [b] Decomposition.

was allowed to cool to 60 °C, and then a distillation assembly was mounted in place of the Soxhlet extractor. The 9-borabicyclo[3.3.1]nonane (250 mL of a 0.5 M solution in dry and degassed THF) was then added dropwise through a syringe. After a few minutes evolution of hydrogen gas started, its volume was measured with a "wet-test meter", and THF was slowly removed by distillation while the gas evolution continued. After 2 h, 3.2 L of H_2 were collected while the temperature was allowed to increase to 140 °C. Then ca. 50 mL of toluene was distilled off and replaced by 100 mL of hexane. The resulting precipitate was removed by filtration, and the residue was washed three times with hot hexane and then dried in vacuo. Recrystallization from THF/hexane afforded 29.2 g (79%) of 1 (mp >240 °C) and 30.2 g (75%) of 2 (mp >250 °C), respectively.

Complexes 4–12. To solutions of the appropriate [$Rh_2Cl_2(LL)_2$] compound (150 mg in 10 mL of CH_3CN) were gradually added at −20 °C 2 equiv of the pyrazolylborate ligands. The mixture was stirred for an additional 1 h while the temperature was allowed to rise to 25 °C. After the solvent was removed in vacuo, the residue was extracted with 50 mL of hexane and the extract filtered through Celite to remove KCl. The hexane was again removed in vacuo, and the resulting product was recrystallised by careful addition of CH_3CN to a CH_2Cl_2 solution and storage at −20 °C for 20 h. Yields, melting points, and analytical data for these complexes are given in Table V.

Analytical Measurements. C, H, and N analyses were performed by the "Mikroelementaranalytisches Laboratorium der Eidgenössischen Technischen Hochschule Zürich".

Physical Measurements. Melting points were obtained from samples in open capillary tubes with a Büchi SMP-20 melting point apparatus, and no corrections were applied. Infrared spectra were recorded in KBr pellets on a Perkin-Elmer Model 883 spectrophotometer.

NMR Spectroscopy. One-dimensional ^1H (500.13/250.13 MHz), ^{13}C (125.7/62.9 MHz), ^{15}N (50.7 MHz), ^{103}Rh (15.8 MHz), and ^{13}C-DEPT[21] and two-dimensional DQF-COSY,[13] NOESY,[12] and HMQC[11] NMR spectra were recorded on Bruker AMX 500 and Bruker WM 250 spectrometers. ^{11}B NMR spectra were obtained at 80.3 MHz on a Bruker AC 250 spectrometer. The chemical shift scales are relative to internal TMS (^1H and ^{13}C) and CH_3NO_2 (^{15}N) and external $BF_3{\cdot}Et_2O$ (^{11}B), whereas ^{103}Rh shifts are on the absolute scale Ξ = 3.16 MHz, whereas TMS resonates at exactly 100 MHz.

Crystallography. Air-stable yellow crystals of [{BBN-(pz)$_2$}Rh(COD)] (6), suitable for X-ray diffraction, were obtained by crystallization from acetonitrile. A prismatic crystal was mounted on a glass fiber at random orientation on an Enraf-Nonius CAD4 diffractometer for unit cell and space group determination and for data collection. Systematic absences were consistent with the orthorhombic space groups *Pna*2 and *Pnma*. The latter, centrosymmetric space group was chosen as (1) it is consistent with the molecular geometry in solution and (2) it required a smaller number of parameters in the least-squares refinement. The choice was later confirmed by the successful refinement.

Table VI. Experimental Data for the X-ray Diffraction Study of [{(C_8H_{14})B(pz)$_2$}Rh(COD)]

formula	$C_{22}H_{32}BN_4Rh$
mol wt	466.24
cryst dimens, mm	0.15 × 0.25 × 0.30
data coll *T*, °C	23
cryst syst	orthorhombic
space group	*Pnma*
a, Å	12.940 (2)
b, Å	13.697 (2)
c, Å	11.959 (2)
V, Å^3	2119.7 (5)
Z	4
ρ_{calcd}, g cm^{-3}	1.460
μ, cm^{-1}	8.07
radiation	Mo Kα (graphite monochromated λ = 0.71069 Å)
measd reflcns	+*h*,+*k*,+*l*
θ range, deg	$2.7 < \theta < 27.0$
scan type	$\omega/2\theta$
scan width, deg	1.10 + 0.35 tan θ
max counting time, s	75
bkdg time, s	0.5 × scan time
max scan speed, deg min^{-1}	5.2
prescan rejection limit	0.55 (1.82σ)
prescan acceptance	0.025 (40.00 σ)
horiz receiving slit, nm	1.70 + tan θ
vert receiving slit, mm	4.0
no. of data coll	2409
no. of obsd reflcns (n_0) ($\lvert F_o\rvert^2 > 3.0\sigma(\lvert F\rvert^2)$)	1485
no. of params refined (n_v)	144
R^a	0.034
$R_w{}^b$	0.041
GOF[c]	1.357

[a] $R = \sum\lvert\lvert F_o\rvert - 1/k\lvert F_c\rvert\rvert/\sum\lvert F_o\rvert$. [b] $R_w = [\sum w(\lvert F_o\rvert - 1/k\lvert F_c\rvert)^2/\sum w\lvert F_o\rvert^2]^{1/2}$, where $w = [\sigma^2(F_o)]^{-1}$ and $\sigma(F_o) = [\sigma^2(I) + (f\text{-}(F_o)^2)^2]^{1/2}/2F_o$ with $f = 0.040$ and $\sigma(I)$ based on counting statistics alone. [c] $\text{GOF} = [\sum w(\lvert F_o\rvert - 1/k\lvert F_c\rvert)^2/(n_o - n_v)]^{1/2}$.

Unit cell dimensions were obtained by least-squares fit of the 2θ values of 25 high-order reflections (9.6° < 2θ < 18.2°) using the CAD4 centering routines. A list of crystallographic and other relevant data are given in Table VI.

Data were collected with variable scan speed to ensure constant statistical precision on the collected intensities. Three standard reflections, used to check the stability of the crystal and of the experimental conditions, were measured every hour; no significant variation was detected. The orientation of the crystal was checked by measuring three reflections every 300 measurements. Data were corrected for Lorentz and polarization factors and for decay, using the data reduction programs of the CAD4-SDP package.[22] An empirical absorption correction was applied by using azimuthal ψ-scans of three "high-χ" angle reflections (χ > 86.9°; 10.7° < 2θ < 15.7°). The standard deviations on intensities were calculated in the term of statistics alone, while those on F_o were calculated

---

(21) Doddrell, D. M.; Pegg, D. T.; Bendall, M. R. *J. Magn. Reson.* 1982, *48*, 323.

(22) *Enraf-Nonius Structure Determination Package, SDP*; Enraf-Nonius: Delft, The Netherlands, 1980.

Table VII. Final Positional Parameters and Equivalent Thermal Parameters (Å^2) for [Rh{(C_8H_{14})B(pz)$_2$}(COD)] (6) (Esd's in Parentheses)[a]

atom	*x*	*y*	*z*	B_{eq}
Rh	0.54732 (4)	0.250	0.13165 (3)	3.876 (8)
N1	0.6380 (2)	0.1446 (2)	0.0489 (2)	3.74 (6)
N2	0.6701 (2)	0.1603 (2)	−0.0579 (2)	3.19 (6)
C1	0.6927 (4)	0.0681 (3)	0.0866 (4)	4.85 (9)
C2	0.7589 (3)	0.0349 (3)	0.0054 (3)	5.5 (1)
C3	0.7430 (3)	0.0949 (3)	−0.0840 (4)	4.43 (8)
C4	0.6595 (4)	0.250	−0.2552 (4)	3.8 (1)
C5	0.6180 (3)	0.1575 (3)	−0.3142 (3)	4.95 (9)
C6	0.5028 (4)	0.1376 (3)	−0.2997 (3)	4.83 (9)
C7	0.4623 (3)	0.1549 (3)	−0.1814 (3)	4.14 (8)
C8	0.5018 (4)	0.250	−0.1266 (4)	3.23 (9)
C9	0.4979 (4)	0.3521 (4)	0.2538 (4)	6.8 (1)
C10	0.4286 (4)	0.3516 (4)	0.1671 (4)	6.2 (1)
C11	0.3252 (5)	0.3031 (4)	0.1682 (6)	9.5 (2)
C12	0.4788 (6)	0.3031 (5)	0.3652 (4)	11.1 (2)
B	0.6235 (4)	0.250	−0.1255 (5)	2.9 (1)
H8	0.477 (3)	0.250	−0.056 (4)	1.1 (9)*
H9	0.557 (3)	0.096 (3)	0.252 (4)	4 (1)*
H10	0.433 (3)	0.401 (3)	0.115 (3)	4 (1)*

[a] Starred atoms were refined isotropically. Anisotropically refined atoms are given in the form of the isotropic equivalent displacement parameter defined as $(^1/_3)[a^2B(1,1) + b^2B(2,2) + c^2B(3,3)]$.

as reported in Table VII. Intensities were considered as observed if $F_o^2 \geq 3.0\sigma(F^2)$ and used for the resolution and refinement of the structure. A value of $F_o = 0.0$ was given to those reflections having negative net intensities. The structure was solved by the combination of Patterson and Fourier methods and refined by full-matrix least-squares procedures (the function minimized was $[\sum w(|F_o| - 1/k|F_c|)^2]$ with $w = [\sigma^2(F_o)]^{-1}$). No extinction correction was deemed to be necessary.

The scattering factors used, corrected for the real and imaginary parts of the anomalous dispersion, were taken from the literature.[23] In the final Fourier difference maps, most of the hydrogens could be located, in particular those bound to C8, C9, and C10. These hydrogen atoms, were considered to be chemically significant and therefore were refined, starting from the experimental coordinates using isotropic temperature displacements. The contribution of the remaining hydrogens, in their idealized positions (C–H = 0.95 Å, *B* = 5.0 Å^2), was taken into account but not refined. Anisotropic temperature factors were used for all non-hydrogen atoms. Upon convergence (no parameter shift of $>0.2\sigma(p)$), the last Fourier difference map showed no significant feature. All calculations were carried out by using the SDP crystallographic package.[22] Final atomic coordinates and equivalent thermal factors are given in Table VII.

Acknowledgment. U.E.B. gratefully acknowledges the support of the "Forschungskommission der ETH Zürich" and A.A. acknowledges financial support from MURST. We thank Prof. P. S. Pregosin for valuable discussion.

Supplementary Material Available: Anisotropic displacement parameters (Table S1), calculated hydrogen positions (Table S2), and an extended list of bond distances and angles (Table S3) for **6** (10 pages). Ordering information is given on any current masthead page.

OM910688B

---

[23] *International Tables for X-ray Crystallography*; Kynoch Press: Birmingham, England, 1974; Vol. IV.

Reactions of the 17-Electron Complex {η^5-$C_5H_5Cr(CO)_3$} with Alkyl Halides

Celeste A. MacConnachie, James M. Nelson, and Michael C. Baird*

Department of Chemistry, Queen's University, Kingston, Ontario, Canada K7L 3N6

Received March 20, 1992

Solutions of the compound [η^5-$C_5H_5Cr(CO)_3$]$_2$ react with a series of organic halides RX (R = Me, $CH_2CH{=}CH_2$, $CH_2CH{=}CHCO_2Me$, CH_2Ph, CH_2CO_2R' (R′ = Me, Et), CH_2CN, $CH(CO_2Me)_2$; X = Br, I) to form the corresponding alkyl- and halochromium compounds η^5-$C_5H_5Cr(CO)_3R$ and η^5-$C_5H_5Cr(CO)_3X$. The new alkylchromium compounds are characterized by elemental analyses where possible, otherwise by spectroscopic techniques and comparisons with the compounds synthesized by reactions of the same alkyl halides with Na[η^5-$C_5H_5Cr(CO)_3$]. In contrast, organic halides containing one or more β-hydrogen atoms, RCH_2CH_2X, react to form η^5-$C_5H_5Cr(CO)_3H$, η^5-$C_5H_5Cr(CO)_3X$, $RCH{=}CH_2$, and RCH_2Me. Since [η^5-$C_5H_5Cr(CO)_3$]$_2$ is known to dissociate spontaneously in solution at ambient temperature to the highly reactive, 17-electron, metal-centered radical species {η^5-$C_5H_5Cr(CO)_3$}, it is suggested that the reactions involve initial halogen abstraction from the alkyl halides by {η^5-$C_5H_5Cr(CO)_3$}, followed, for alkyl halides containing no β-hydrogen atoms, by coupling of the resulting alkyl radical with a second molecule of {η^5-$C_5H_5Cr(CO)_3$}. For alkyl halides containing β-hydrogen atoms, analyses of product distributions are consistent with initial halogen abstraction by {η^5-$C_5H_5Cr(C0)_3$} from RCH_2CH_2X followed by H-atom abstraction from $RCH_2CH_2^{\bullet}$ to give η^5-$C_5H_5Cr(CO)_3H$ and olefin. As the concentration of η^5-$C_5H_5Cr(CO)_3H$ increases, a secondary process, in which the radical $RCH_2CH_2^{\bullet}$ abstracts an H-atom from η^5-$C_5H_5Cr(CO)_3H$, becomes competitive. Observed coalescence of the η^5-C_5H_5 ^{1}H NMR resonance of [η^5-$C_5H_5Cr(CO)_3$]$_2$ with those of η^5-$C_5H_5Cr(CO)_3X$ (X = H, Br, I) is interpreted in terms of facile X-atom exchange which also proceeds via X-atom abstraction processes by [η^5-$C_5H_5Cr(CO)_3$}.

Although organotransition metal chemistry has long been dominated by compounds containing closed-shell, 18-electron configurations,[1] recent years have seen the development of a very extensive chemistry of electronically unsaturated, 17-electron complexes.[2] While most known examples of the latter class of paramagnetic, metal-centered radicals are unstable with respect to a wide variety of coupling, atom abstraction and disproportionation re-

---

[1] Collman, J. P.; Hegedus, L. S.; Norton, J. R.; Finke, R. G. *Principles and Applications of Organotransition Metal Chemistry*; University Science Books: Mill Valley, CA, 1987.

[2] (a) Baird, M. C. *Chem. Rev.* 1988, *88*, 1217. (b) Trogler, W. C., Ed. *Organometallic Radical Process*; Elsevier: Amsterdam, 1990.

0276-7333/92/2311-2521$03.00/0 © 1992 American Chemical Society